Endothelial cell-related autophagic pathways in a severe pulmonary hypertension model

(重症肺高血圧症モデルにおける肺血管内皮細胞動態とオートファジーの役割)

千葉大学大学院医学薬学府

先端医学薬学専攻

(主任：巽 浩一郎 教授)

加藤 史照

Title

Endothelial cell-related autophagic pathways in a severe pulmonary hypertension model

Author

Fumiaki Kato, MD

Department of Respirology, Graduate School of Medicine, Chiba University, Chiba, Japan

Running Head: Endothelial cell-related autophagy in pulmonary hypertension

Corresponding author and address for reprints requests:

Fumiaki Kato, MD.

Department of Respirology, Graduate School of Medicine, Chiba University, 1-8-1 Inohana, Chuou-ku, Chiba 260-8670, Japan.

Abstract

Introduction

Pulmonary arterial hypertension (PAH) is characterized by progressive obstructive remodeling of the pulmonary arteries. No report has shown a causative role of the autophagic pathway in the progression of pulmonary vascular endothelial cell (EC) alterations in PAH. The aims of this study were to investigate the time-dependent role of the autophagic pathway in pulmonary vascular ECs as well as pulmonary vascular EC kinesis in a severe PAH rat model (Sugen/Hypoxia rat) and to confirm whether timely induction of the autophagic pathway by rapamycin results in the improvement of PAH.

Methods

Hemodynamic and histological examinations and a flow cytometry analysis of the EC-related autophagic pathways and pulmonary vascular EC kinetics with the lung cell suspension were performed. Additionally, the autophagic pathway was induced in a timely manner by rapamycin and its therapeutic effects were assessed.

Results

The right ventricular systolic pressure (RVSP) and the obstructive vessels due to pulmonary vascular remodeling increased. The expression of autophagic marker LC3 in

ECs was altered in a time-dependent manner, in parallel with proliferation and apoptotic markers. Crosstalk between pulmonary vascular remodeling and the autophagic pathway, especially in small vascular lesions, was suggested. Moreover, rapamycin activated the autophagic pathway and improved cell proliferation and apoptosis balance in pulmonary vascular ECs, resulting in reduction of RVSP and pulmonary vascular remodeling.

Conclusion

The pulmonary vascular EC-related autophagic pathway is altered in a time-dependent manner and activation of the autophagic pathway due to rapamycin may have a beneficial role on ameliorating pulmonary arterial remodeling and the hemodynamics.

Introduction

Pulmonary arterial hypertension (PAH) is characterized by not only increased pulmonary arterial vascular tone, but also progressive obstructive remodeling of the pulmonary arteries, both of which lead to increased pulmonary vascular resistance, right ventricular failure and death (5, 13, 26). These vascular alterations involve marked proliferation of pulmonary artery endothelial cells (ECs) and smooth muscle cells (22, 32). Furthermore, it was also reported that these cells in angioproliferative vascular lesions had some neoplastic features (27, 30, 31). It is generally acknowledged that the current vasodilative drugs, i.e., prostacyclin and its analogs, phosphodiesterase type 5 inhibitors and endothelin receptor blockers, have not only vasodilative effects, but also antiproliferative effects on phenotypically altered cells (2, 17, 35, 40). However, these drugs alone do not appear to be sufficient for reversing the vasoobliterative lesions (33, 37). In fact, it has been demonstrated that, in the PAH rat model, therapeutic intervention with macitentan (an endothelin receptor antagonist) can decrease an elevated pulmonary artery pressure to some extent, but not reverse the vascular lesions completely (36). Therefore, in addition to current vasodilator drugs, drugs which can reverse remodeling of the vasoobliterative lesions are needed for the superior treatment of severe PAH patients.

In recent years, autophagy has attracted much attention because it appears to play essential roles in many different pathological conditions including PAH (14). Autophagy is a catabolic mechanism involving the degradation of intracellular proteins and organelles, resulting in the supply of amino acids to be recycled for the synthesis of essential proteins corresponding to their own conditions (23). During this process, cytoplasmic proteins and organelles are engulfed by double-membrane-bound structures (autophagosomes) and these structures are fused with lysosomes/vacuoles for degradation. The microtubule-associated protein light chain-3 (LC3), which is an important molecule for autophagosome transport and maturation, has been widely used to monitor autophagy (23). There are some *in vitro* experiments that suggest correlations between the autophagic pathway and pathobiology in the development of PAH. (14) In addition, a recent paper suggested that an accelerated autophagic pathway, which was assessed by elevated LC3 expression levels, may play a role not only in the rodent model of PH, but also in patients with PAH (18).

The mammalian target of rapamycin (mTOR), which has been recognized as one of several protein kinases that regulate autophagy, has been the most studied (15). Rapamycin is an antiproliferative immune suppressor that induces cell arrest and an inhibitor of mTOR (4). It has been shown that rapamycin has a role in inhibiting

hypoxia-induced activation of pulmonary arterial adventitial fibroblasts (7) and also has an effect of antiproliferation on pulmonary arterial smooth muscle cells isolated from organized thrombus in patients with chronic thromboembolic pulmonary hypertension (25). In fact, rapamycin has been shown to reduce right ventricular (RV) systolic pressure (RVSP) and inhibit medial thickness in monocrotaline-induced PH models (12). These results suggest that an accelerated autophagic pathway with rapamycin may have beneficial therapeutic effects on hyperproliferative and activated cells observed in PH. However, in monocrotaline models, there was no obliterative and stenosed intimal lesions with phenotypically altered proliferated endothelial-like cells, which are believed to be characteristic lesions of human PAH, and their defining pulmonary vascular lesions appear to be medial thickness with proliferating smooth muscle cells (33). Although a recent *in vitro* study demonstrated that rapamycin reduced the migration of ECs derived from human pulmonary artery (28), it remains unknown whether autophagy induction due to rapamycin plays an actual role in controlling phenotypical altered endothelial-like cells.

It has been demonstrated that in rodent models of PH plexiform-like lesions, which are known to be characteristic of PAH, develop only in the Sugen/Hypoxia model. In this rat model, a single percutaneous injection of a vascular endothelial growth factor

receptor blocker (SU5416) in combination with chronic exposure to hypoxia results in severe PAH (1, 39). Pulmonary vascular lesions including all features described in the Heath-Edwards classification (11) also appeared in a time-dependent manner (1, 39). Furthermore, specific to this model, medial muscular thickening of proliferating smooth muscle cells and intimal obliteration with phenotypically altered proliferated ECs are observed (1, 26, 39). Thus the Sugen/Hypoxia model appears to be an appropriate model to examine the EC kinetics *in vivo*.

To the best of our knowledge, there is no report which shows a causative role of the autophagic pathway in the progression of pulmonary vascular EC alterations in PAH, especially in a time-dependent manner. The aims of this study were to investigate the time-dependent role of the autophagic pathway in pulmonary vascular ECs using the Sugen/Hypoxia model and to confirm whether timely induction of the autophagic pathway with rapamycin results in an improvement in pulmonary vascular remodeling and the hemodynamics.

Materials and Methods

Experimental protocols and animals.

Two experiments were conducted: (A) the time course study and (B) the

interventional study. The procedure of (A), the time course study, is outlined in Figure (Fig.) 1A. To prepare the Sugen/Hypoxia model, five-week-old male Sprague-Dawley (SD) rats (CLEA Japan, Tokyo, Japan) weighing 100 to 140 g were injected subcutaneously with SU5416 (30 mg/kg; Cayman, Ann Arbor, MI, USA), which was suspended in carboxyl cellulose comprising 0.5% [wt/vol] carboxymethylcellulose sodium, 0.9% [wt/vol] NaCl, 0.4% [vol/vol] polysorbate, and 0.9% [vol/vol] benzyl alcohol in deionized water, and exposed to normobaric hypoxia (10% O_2) for 3 weeks as previously reported with minor modifications (1). These animals were subsequently returned to normoxia (21% O_2) for up to 5 weeks. Five-week-old male SD rats were also exposed to normoxia for 8 weeks as normal controls. All rats had free access to food and water. We examined 4 groups of Sugen/Hypoxia rats sacrificed at 1, 3, 5, 8 weeks after SU5416 injection, and 1 group of control rats at 5 weeks after SU5416 injection. In a flow cytometry (FCM) analysis, 4 control groups at 1, 3, 5, and 8 weeks were matched and examined with the respective groups of Sugen/Hypoxia rats. The procedure of (B), the interventional protocol, is outlined in Fig. 1B. Sugen/Hypoxia rats were prepared as described previously (1) and we examined the effects of rapamycin (LC laboratories, Woburn, MA, USA). Rapamycin was dissolved in a vehicle containing 5.2% [vol/vol] Tween-80 and 5.2% [vol/vol] polyethylene glycol 400

(41). In this protocol, Sugen/Hypoxia rats were intraperitoneally administered either rapamycin 5 mg/kg or vehicle 3 times per week for 5 weeks starting 3 weeks after SU5416 injection. Each group was examined at 8 weeks after SU5416 injection. All animal procedures were conducted under protocols approved by the Review Board for animal experiments of Chiba University.

Hemodynamic Measurements in Catheterized Rats

Hemodynamic measurements were performed as previously reported with slightly modifications (1). Rats were intraperitoneally anesthetized with pentobarbital sodium (30 mg/kg). Hemodynamic measurements were performed under normoxic conditions. Polyethylene tube catheters (size 3, outer diameter 1.0 mm; Hibiki, Tokyo, Japan) were inserted into the right ventricle through the right jugular vein in order to measure the RVSP and heart rate (HR). The signals were monitored with a physiological transducer (NEC Sanei Co., Ltd. Tokyo, Japan), an amplifier system (NEC Sanei Co., Ltd. Tokyo, Japan) and a recorder (Nihon Kohden, Tokyo, Japan). After hemodynamic measurements, the rats were euthanized with pentobarbital sodium (150 mg/kg). The lungs and hearts were harvested for histological, immunohistochemical and FCM analyses. The weights of the RV and left ventricle

(LV) + septal (S) were measured for the RV/LV+S ratio.

Histological and immunohistochemical procedure

Tissue preparation

Lung tissues were inflated and fixed with 4% paraformaldehyde at 4°C for more than 48 hours. The right upper lobes were embedded with paraffin. Sections were cut at 2 μm.

Histological procedure

The lung sections were deparaffinized in xylene, hydrated using ethanol, and stained with Elastica van Gieson (EVG) stain using standard protocols for morphological analyses.

Immunohistochemical procedure

The lung sections were deparaffinized in xylene and hydrated using ethanol. The slides were boiled in pH 6.0 citrate buffer (Abcam, Cambridge, UK) for 10 minutes, blocked with Block Ace (Dainippon Sumitomo Pharma, Tokyo), and incubated with the anti-von Willebrand factor (vWF) antibody (Abcam, Cambridge, UK; x100) and

anti-LC3 antibody (Medical & Biological Laboratories, MBL, Nagoya, Japan; x400) at 37°C for 60 minutes. After primary incubation, the sections were incubated with secondary antibodies (Histofine Simple Stain MAX PO; Nichirei, Tokyo, Japan) at 37°C for 30 minutes. Peroxidase activity was detected with diaminobenzidine (DAB; Simple Stain DAB chromogen; Nichirei, Tokyo, Japan) and counterstained with hematoxylin and dehydrated.

Morphological/Histological Analyses

Pulmonary arterial occlusive rates were evaluated as previously reported (39) with slight modifications. All arteries in 1 slice of each right upper lobe were counted. The arteries were analyzed at x400 and representative photomicrographs were shown at x1000.

The arteries were divided into 3 groups according to the size of the outer diameter (OD) as following: OD < 50 μm, 50 μm < OD < 100 μm, OD > 100 μm. In each group, the arteries on the EVG stain were scored depending on the luminal occlusive rate as follows: no evidence of neointimal formation (grade 0); partial (< 50%) luminal occlusion (grade 1); and severe (> 50%) luminal occlusion (grade 2). Grade 2 arteries were additionally classified into 2 patterns according to

immunostaining with vWF as follows: the non-plexiform pattern in which vWF-positive cells were only circularly lined on the innermost layer (non-plexiform type), or the plexiform pattern in which vWF-positive cells formed a complex/disorganized plexus/channel-like pattern.

The arteries were additionally classified into 2 groups according to immunostaining with LC3. The arteries in which > 50% of the innermost layer had LC3-positive cells were defined as LC3-positive arteries. The other arteries were defined as LC3-negative arteries.

After the arteries were counted, the percentage was calculated.

Flow cytometry analysis

Bromodeoxyuridine labeling for the detection of proliferating cells

Bromodeoxyuridine (BrdU; Sigma-Aldrich, St. Louis, MO, USA) is a thymidine analog incorporated into DNA of actively proliferating cells during the S-phase of the cell cycle. BrdU was used to detect cell proliferation on FCM. Twelve and 24 hours before the assay, the rats were intraperitoneally injected with 50 mg/kg of BrdU in phosphate-buffered saline (PBS) as previously reported with slight modifications (24).

Lung single-cell suspensions

For the FCM analysis, lung cell suspensions performed as previously reported (24). The left upper lungs were minced using scissors and subjected to enzymatic digestion: Dulbecco`s modified Eagle medium (DMEM; Sigma-Aldrich) containing 1% bovine serum albumin (BSA; Wako, Osaka, Japan), 2 mg/ml collagenase (Wako, Osaka, Japan), 2.5 mg/ml Dispase II (Roche Diagnostics, Mannheim, Germany), and 125 μg/ml DNase (Wako, Osaka, Japan). The suspensions were incubated at 37°C on a shaker for 60 minutes and then filtered through a 100 μm nylon mesh screen. After dispersion of the lung cells, the total number of cells was counted.

Flow cytometry analysis

FCM was performed as previously reported (24). The digested lung cells were pretreated with anti-CD32 antibody (BioLegend, San Diego, CA, USA) to block Fc receptors and then stained with a mixture of fluorophore-conjugated antibodies in the dark at 4°C for 30 minutes. The following anti-rat antibodies were used: FITC-conjugated anti-CD31 (Abcam, Cambridge, UK), Alexa Fluor 700-conjugated anti-CD45 (BioLegend). To measure DNA degradation, some cells were incubated

with 10 μg/ml of Hoechst 34580 (Life Technologies, Grand Island, NY, USA) for 25 minutes at room temperature (RT). After fixation with BD Cytofix/Cytoperm™ Plus (BD Pharmingen, San Jose, CA, USA), the following anti-rat antibodies were used: PE-conjugated anti-LC3 (Cell Signaling Technology, Tokyo, Japan) at RT 60 minutes and APC-conjugated anti-BrdU (BD Pharmingen) at RT for 35 minutes. Irrelevant isotype-matched antibodies were used as controls. We took 1×10^6 cells per sample and 1.5×10^5 events were recorded using a flow cytometer (FACS Canto™ II; BD Biosciences, San Jose, CA, USA). The FCM data were analyzed using the FlowJo software program (Tree Star, San Carlos, CA, USA).

Statistical analysis

Quantitative data are presented as the means ± standard error of means. Comparisons among the groups were made using Student's *t*-test or one-way ANOVA (followed by Tukey's multiple comparisons test). P values < 0.05 were considered to be statistically significant. Statistical analyses were performed using the GraphPad Prism version 6 software program (GraphPad Software Inc., La Jolla, CA, USA).

Result

Baseline hemodynamics and RV hypertrophy

The RVSP increased in a time-dependent manner and peaked at 8 weeks after SU5416 injection (Fig. 2A). RV hypertrophy was observed in Sugen/Hypoxia rats from 3 weeks after SU5416 injection when compared with control rats (Fig. 2B). No significant difference was observed in the HR (Fig. 2C). The body weight data are shown in Fig. 2D.

Pulmonary arterial occlusion

A total of 1,679 arteries were assessed in 24 right upper lobes from 5 groups during the time course study (n=4 each). The result of the pulmonary arterial grading analyses is shown in Fig. 3A-D. Representative photomicrographs of the pulmonary arteries are shown in Fig. 3E-H. A grade 0 artery is demonstrated in Fig. 3E, grade 1 in Fig. 3F, and grade 2 in Fig. 3G, 3H stained by EVG. In grade 2, non-plexiform type arteries are shown in Fig. 3I, 3J and arteries of plexiform type in Fig. 3K, 3L stained by vWF. In OD < 50 μm arteries, the rates of grades 1 and 2 significantly increased at 1, 3, 5 and 8 weeks, and 5 and 8 weeks after SU5416 injection, respectively (Fig. 3A). The rate of plexiform type arteries significantly increased at 8 weeks in OD < 50 μm arteries (Fig. 3B). In 50 μm < OD <100 μm arteries, the rate of grade 1 significantly

increased at 5 weeks (Fig. 3C). There was no evidence that the rate of grade 2 arteries or plexiform type increased in 50 μm < OD < 100 μm arteries (Fig. 3C, 3D). OD > 100 μm arteries were all classified into grade 0 (data not shown).

Pulmonary vascular EC kinetics and initially increase of LC3 positive ECs in FCM analysis

Three left upper lobes of lungs were assessed in each group. FCM was used for the analyses of EC kinetics. The representative FCM panels and gating are shown in Fig. 4A-D. CD31-positive and CD45-negative cells were defined as ECs in the FCM analysis (Fig. 4A). For the assessment of LC3-positive ECs, an area gated to include less than 0.1% of the ECs in the isotype control was used for LC3 evaluation because the distribution of LC3-positive cells continuously changed (Fig. 4B). The positive rates of BrdU, as an indicator of cell proliferation, and Hoechst < 2n (nuclear stain with less than diploidy), as that of cell apoptosis, were also assessed in the ECs (Fig. 4C, 4D). The results are shown in Fig. 4E-I. The LC3-positive rate was significantly higher from 1 to 3 weeks in the Sugen/Hypoxia rats than the controls (Fig. 4E). Additionally, LC3-positive ECs increased more in the Sugen/Hypoxia rats than in the control and only hypoxia exposure groups (Fig. 4F). The BrdU-positive rate in

ECs from Sugen/Hypoxia rats significantly increased at 1, 5 and 8 weeks after SU5416 injection when compared with the controls, with a particularly high rate at 1 week (Fig. 4G). The rate of Hoechst < 2n in the ECs from the Sugen/Hypoxia rats decreased from 5 to 8 weeks after SU5416 injection (Fig. 4H). The number of ECs, which was corrected by body weight, was higher in the Sugen/Hypoxia rats than in the controls over the entire period (Fig. 4I).

LC3 changes were dominant in small pulmonary arteries

Immunostaining was performed to observe the localization of LC3-positive cells. Representative photomicrographs of pulmonary arteries which were immunostained with LC3 are shown in Fig. 5A-D. LC3-positive arteries are shown in Fig. 5A-B and LC3-negative arteries are shown in Fig. 5C-D. In OD < 50 μm arteries, the rate of LC3-positive arteries in the Sugen/Hypoxia rats was higher than in the controls (Fig. 5E). There was no statistically significant difference between the control and PAH model vessels in 50 μm < OD < 100 μm and OD > 100 μm arteries (Fig. 5F, 5G). The rate of LC3-positive arteries in OD < 50 μm tended to increase more than in the other OD groups, especially at 1 and 3 week after SU5416 injection (Fig. 6A, 6B) where increased LC3-positive ECs were observed in the FCM analysis (Fig. 4E).

Effects of rapamycin on the hemodynamics and RV hypertrophy

Because the FCM analysis demonstrated that a decrease in LC3-positive ECs started from 3 weeks after SU5416 injection (Fig. 4E), the Sugen/Hypoxia rats were treated with rapamycin to activate the autophagic pathway from 3 to 8 weeks after SU5416 injection.

The results in the hemodynamics and other parameters at 8 weeks after SU5416 injection are shown in Fig. 7A-D. The RVSP and HR were significantly decreased in rapamycin-treated Sugen/Hypoxia rats when compared with vehicle-treated Sugen/Hypoxia rats (Fig. 7A, 7B). There was only a tendency towards a decrease in the RV/LV+S ratio in rapamycin-treated Sugen/Hypoxia rats when compared with vehicle-treated Sugen/Hypoxia rats (Fig. 7C). Additionally, the body weight was significantly lower in the rapamycin-treated Sugen/Hypoxia rats (Fig. 7D).

Effects of rapamycin on endothelial cells assessed by the FCM analysis

The effects of rapamycin on ECs assessed by the FCM analysis are shown in Fig. 7E-H. The rate of LC3-positive, BrdU-positive, and Hoechst < 2n ECs were compared between rapamycin- and vehicle-treated Sugen/Hypoxia rats at 8 weeks, and

the number of ECs corrected by body weight was also calculated. An increase in LC3-positive cells, a decrease in BrdU-positive cells and an increase in Hoechst < 2n cells was observed in rapamycin-treated Sugen/Hypoxia rats (Fig. 7E-G). There was no significant difference in the number of ECs corrected by body weight between the groups (Fig. 7H).

Effects of rapamycin on pulmonary arteries assessed by an immunohistological analysis with LC3 staining

The rates of LC3-positive arteries assessed by an immunohistological analysis were compared between rapamycin- and vehicle-treated Sugen/Hypoxia rats at 8 weeks (Fig. 7I-K). A higher rate of LC3-positive arteries in OD < 50 μm was observed in rapamycin-treated Sugen/Hypoxia rats (Fig. 7I). There was no significant difference in those in 50 μm < OD < 100 μm or OD > 100 μm arteries between the groups (Fig. 7J, 7K). Representative photomicrographs of pulmonary arteries immunostained with LC3 are shown in Fig. 7L-O (Fig. 7L and 7M, LC3-negative arteries from vehicle-treated Sugen/Hypoxia rats; Fig. 7N and 7O, LC3-positive arteries from rapamycin-treated Sugen/Hypoxia rats).

Effects of rapamycin on pulmonary vascular remodeling

A total of 660 arteries were assessed in 8 right upper lobes from rapamycin- and vehicle-treated Sugen/Hypoxia rat groups (n=4 each). The effects of rapamycin on pulmonary vascular alterations are shown in Fig. 8. In OD < 50 μm arteries, the rates of grade 1, 2 and plexiform type in rapamycin-treated Sugen/Hypoxia rats were significantly lower than those in vehicle-treated Sugen/Hypoxia rats at 8 weeks (Fig. 8A, 8B). In 50 μm < OD < 100 μm arteries, the rate of grade 1 in rapamycin-treated Sugen/Hypoxia rats was significantly lower than those in vehicle-treated Sugen/Hypoxia rats (Fig. 8C). There was no significant difference in the rates of plexiform type in 50 μm < OD < 100 μm arteries between the groups (Fig. 8D). Representative photomicrographs of pulmonary arteries stained with EVG are shown in Fig. 8E-H (Fig. 8E and 8F, lungs from vehicle-treated Sugen/Hypoxia rats; Fig. 8G and 8H, lungs from rapamycin-treated Sugen/Hypoxia rats).

Discussion

The current study demonstrated pulmonary vascular EC-related autophagic alterations in a time-dependent manner (Fig. 4E), parallel with proliferation (Fig. 4G) and apoptosis (Fig. 4H), and LC3 expression in the pulmonary vasculature (Fig 5A-C)

in a rat model of severe PAH. Moreover, this is the first study to confirm the roles of rapamycin as an autophagy activator in reducing RVSP (Fig. 7A), ameliorating pulmonary arterial remodeling (Fig. 8A-C), and activating autophagy in ECs (Fig. 7E). The current study demonstrated that the balance between proliferation and apoptosis of pulmonary vascular ECs was dysregulated in the Sugen/Hypoxia rat model (Fig. 4E, G, H). Excess activation of autophagy has been shown to result in cell death, i.e., autophagic cell death (20). A decreased number of LC3-positive ECs from 3 weeks (Fig. 4E), in parallel with a decrease in Hoechst < 2n cells (Fig. 4H), thus suggested the appearance of apoptosis-resistant ECs, as shown in the previous report (29, 38). However, there was a marked increase in BrdU-positive ECs, especially at 1 week after SU5416 injection (Fig. 4G), despite the appearance of obstructive and/or stenosed intimal lesions composed of proliferative cells and the progression of pulmonary vascular remodeling (Fig. 3A-C). Although this result did not support our previous data from an *in vitro* experiment (29), recent papers have demonstrated that, in the Sugen/Hypoxia rat model, most of the proliferative cells comprising intimal lesions were negative for EC markers (36) and these EC marker-negative cells were suggested to originate from ECs through the endothelial-to-mesenchymal transition (EndMT) in human PAH and the Sugen/Hypoxia rat model (28). In the current study, a decrease in

the number of BrdU-positive ECs from 3 weeks after SU5416 injection may be partially attributable to the EndMT. Previously, Lee et al. showed that an increased expression of autophagic protein LC3 exerted a protective function against PH progression in the chronic hypoxia mice model (18). However, this model has been acknowledged to develop only mild to moderate PH with medial thickening of proliferative pulmonary arterial smooth muscle cells, which lack plexiform-like lesions composed of phenotypically altered proliferated ECs (32). In the present study, an increased expression of autophagic protein LC3 in the ECs was observed (Fig. 4E) and the induction of the autophagic pathway by rapamycin had a role in reversing pulmonary vascular remodeling in the Sugen/Hypoxia rat model (Fig. 8A-D), suggesting that the autophagic pathway exerts a protective function not only in the medial lesions, but also in the complex vascular lesions including plexiform-lesions and intimal lesions, which have been demonstrated in the Sugen/Hypoxia rat model. Moreover, an expression of autophagic protein LC3 predominantly increased in the peripheral arteries (Fig. 5E) in accordance with pulmonary vascular remodeling (Fig. 3A-D). The time-dependent alteration in pulmonary vascular remodeling also appeared to be in parallel with the RVSP (Fig. 2A, 3A). These results suggest that the autophagic pathway plays a roll especially in the peripheral arteries, which might be attributable to the progression of

pulmonary hemodynamics (6, 24, 39).

The current study showed that the LC3 expression initially increased and eventually decreased in a time-dependent manner (Fig 4E, 5E). Autophagy is a catabolic mechanism for cells to maintain homeostasis under stressed conditions (23). The dysregulated autophagic pathway is shared between cancer and pulmonary vascular cells in PAH (9, 18). In fact, the activated and inactivated autophagic pathways are believed to have a role in cancer cell growth and regression (19). However, it remains unknown whether autophagy is beneficial or harmful in the progression of pulmonary vascular lesions. As shown in a previous report (18), a protective function of the autophagic pathway against PH progression through its induction by rapamycin has been shown in the current study, especially during the period of decreased LC3 expression. An initial increase in LC3 expression in ECs until 3 weeks may represent autophagic cell death under a stressed environment induced by SU5416 injection and chronic hypoxia. In parallel with reducing the apoptotic cell marker (Fig. 4H), a decreased expression of the autophagic marker initiated at 3 weeks (Fig. 4E) may indicate an appearance of apoptosis-resistant cells. Therefore, rapamycin as an autophagic inducer, i.e., autophagic cell death inducer, might have a reverse effect on the pulmonary vasculature, especially during the period with decreased LC3 expression.

From this point of view, autophagic activation appears to be beneficial and may impact regression of the pulmonary lesions, especially during select periods. Therefore, rapamycin may play a potential role in PAH treatment through EC-related autophagic pathways under restricted conditions.

As demonstrated above, an initial increase in the LC3 expression in ECs appears to be attributable to the stressed environment induced by SU5416 injection and a hypoxic condition. Fig. 4F indicated, however, that the combination of SU5416 injection and a hypoxic condition are essential to induce LC3 expression in ECs.

In the current study, although rapamycin treatment at a dose of 5 mg/kg (3 times per week) (41) showed a beneficial effect in a severe angioproliferative PAH model, the same appropriate dose of this drug may cause adverse effects in patients with PAH because the clinical dose is approximately 0.04 mg/kg (2 mg/body, daily). It was previously reported *in vitro* that high doses of rapamycin (500 nM) had both antiproliferative and proapoptotic effects, while the doses used for clinical applications (20 nM) had a cytostatic function with no appreciable proapoptotic effect in pulmonary arterial smooth muscle cells (8, 12, 16). The beneficial effect of rapamycin in the rat PAH model in this study might be due to high doses of rapamycin. In fact, rapamycin treatment caused growth inhibition in the rapamycin-administered group (Fig. 7D).

Regarding the treatment of human PAH, the optimal dosage and precise administration methods of rapamycin must be further investigated.

It is generally known that rapamycin inhibits the mTOR signaling pathway, which inhibits autophagy, resulting in the activation of the autophagic pathway. However, mTOR functions as a central regulator in the signaling pathways of proliferation and survival of pulmonary vascular cells and in the development of pulmonary vascular remodeling in the experimental PAH model (9). mTOR consists of two distinct multiprotein complexes, mTOR complex (mTORC) 1 and mTORC2, and rapamycin predominantly inhibits mTORC1 (9). Rapamycin results in the activation of the autophagic pathway because mTORC1 suppresses autophagy (10). However, the mTORC1 signaling pathway regulates cell metabolism, cell growth, proliferation and autophagy. Rapamycin potentially inhibits all of these processes via mTORC1 and likely has an antiproliferative effect regardless of the autophagic pathway. In this study, it remains unknown whether only the autophagic pathway played a role in the beneficial effect of rapamycin in the Sugen/Hypoxia PAH model. Interestingly, the proapoptotic effect was observed in pulmonary vascular ECs in the rapamycin-administered group. This effect has not been reported in the mTORC1 pathway. In only ECs other than pulmonary vascular ECs, a few reports have shown

that rapamycin has an apoptotic effect via the mTORC2 pathway (3, 21, 34). This proapoptotic effect is therefore believed to result in autophagic cell death.

Conclusion

The current study demonstrated that, in the Sugen/Hypoxia rat model, the pulmonary vascular EC-related autophagic pathway was altered in a time-dependent manner and the activation of the autophagic pathway due to rapamycin may thus play a beneficial role in ameliorating pulmonary arterial remodeling and hemodynamics.

Acknowledgments

We are grateful to Ikuko Sakamoto, Akiko Moriya, Yoko Sumiya, Tomoko Misawa and Saori Hiruta for their technical assistance with the experiments, and Chieko Handa and Tamie Hirano for their important contributions in the preparation of the manuscript.

References

1. **Abe K, Toba M, Alzoubi A, Ito M, Fagan KA, Cool CD, Voelkel NF, McMurtry IF, and Oka M**. Formation of plexiform lesions in experimental severe pulmonary arterial hypertension. *Circulation* 121: 2747-2754, 2010.

2. **Akagi S, Nakamura K, Matsubara H, Kusano KF, Kataoka N, Oto T, Miyaji K, Miura A, Ogawa A, Yoshida M, Ueda-Ishibashi H, Yutani C, and Ito H**. Prostaglandin I2 induces apoptosis via upregulation of Fas ligand in pulmonary artery smooth muscle cells from patients with idiopathic pulmonary arterial hypertension. *International journal of cardiology* 165: 499-505, 2013.

3. **Barilli A, Visigalli R, Sala R, Gazzola GC, Parolari A, Tremoli E, Bonomini S, Simon A, Closs EI, Dall'Asta V, and Bussolati O**. In human endothelial cells rapamycin causes mTORC2 inhibition and impairs cell viability and function. *Cardiovascular research* 78: 563-571, 2008.

4. **Brown EJ, Albers MW, Shin TB, Ichikawa K, Keith CT, Lane WS, and Schreiber SL**. A mammalian protein targeted by G1-arresting rapamycin-receptor complex. *Nature* 369: 756-758, 1994.

5. **Davie NJ, Schermuly RT, Weissmann N, Grimminger F, and Ghofrani HA**. The science of endothelin-1 and endothelin receptor antagonists in the management of pulmonary arterial hypertension: current understanding and future studies. *European journal of clinical investigation* 39 Suppl 2: 38-49, 2009.

6. **de Raaf MA, Schalij I, Gomez-Arroyo J, Rol N, Happe C, de Man FS, Vonk-Noordegraaf A, Westerhof N, Voelkel NF, and Bogaard HJ**. SuHx rat model: partly reversible pulmonary hypertension and progressive intima obstruction. *The European respiratory journal* 44: 160-168, 2014.

7. **Gerasimovskaya EV, Tucker DA, and Stenmark KR**. Activation of phosphatidylinositol 3-kinase, Akt, and mammalian target of rapamycin is necessary for hypoxia-induced pulmonary artery adventitial fibroblast proliferation. *Journal of applied physiology (Bethesda, Md : 1985)* 98: 722-731, 2005.

8. **Goncharov DA, Kudryashova TV, Ziai H, Ihida-Stansbury K, DeLisser H, Krymskaya VP, Tuder RM, Kawut SM, and Goncharova EA**. Mammalian target of rapamycin complex 2 (mTORC2) coordinates pulmonary artery smooth muscle cell metabolism, proliferation, and survival in pulmonary arterial hypertension. *Circulation* 129: 864-874, 2014.

9. **Goncharova EA**. mTOR and vascular remodeling in lung diseases: current challenges and therapeutic prospects. *FASEB journal : official publication of the Federation of American Societies for Experimental Biology* 27: 1796-1807, 2013.

10. **Hands SL, Proud CG, and Wyttenbach A**. mTOR's role in ageing: protein synthesis or autophagy? *Aging* 1: 586-597, 2009.

11. **Heath D, and Edwards JE**. The Pathology of Hypertensive Pulmonary Vascular Disease: A Description of Six Grades of Structural Changes in the Pulmonary Arteries with Special Reference to

Congenital Cardiac Septal Defects. *Circulation* 18: 533-547, 1958.

12. **Houssaini A, Abid S, Mouraret N, Wan F, Rideau D, Saker M, Marcos E, Tissot CM, Dubois-Rande JL, Amsellem V, and Adnot S**. Rapamycin reverses pulmonary artery smooth muscle cell proliferation in pulmonary hypertension. *American journal of respiratory cell and molecular biology* 48: 568-577, 2013.

13. **Humbert M, Morrell NW, Archer SL, Stenmark KR, MacLean MR, Lang IM, Christman BW, Weir EK, Eickelberg O, Voelkel NF, and Rabinovitch M**. Cellular and molecular pathobiology of pulmonary arterial hypertension. *Journal of the American College of Cardiology* 43: 13s-24s, 2004.

14. **Jin Y, and Choi AM**. Cross talk between autophagy and apoptosis in pulmonary hypertension. *Pulmonary circulation* 2: 407-414, 2012.

15. **Klionsky DJ, and Emr SD**. Autophagy as a regulated pathway of cellular degradation. *Science (New York, NY)* 290: 1717-1721, 2000.

16. **Krymskaya VP, Snow J, Cesarone G, Khavin I, Goncharov DA, Lim PN, Veasey SC, Ihida-Stansbury K, Jones PL, and Goncharova EA**. mTOR is required for pulmonary arterial vascular smooth muscle cell proliferation under chronic hypoxia. *FASEB journal : official publication of the Federation of American Societies for Experimental Biology* 25: 1922-1933, 2011.

17. **Kunichika N, Landsberg JW, Yu Y, Kunichika H, Thistlethwaite PA, Rubin LJ, and Yuan JX**. Bosentan inhibits transient receptor potential channel expression in pulmonary vascular myocytes. *American journal of respiratory and critical care medicine* 170: 1101-1107, 2004.

18. **Lee SJ, Smith A, Guo L, Alastalo TP, Li M, Sawada H, Liu X, Chen ZH, Ifedigbo E, Jin Y, Feghali-Bostwick C, Ryter SW, Kim HP, Rabinovitch M, and Choi AM**. Autophagic protein LC3B confers resistance against hypoxia-induced pulmonary hypertension. *American journal of respiratory and critical care medicine* 183: 649-658, 2011.

19. **Levine B, and Kroemer G**. Autophagy in the pathogenesis of disease. *Cell* 132: 27-42, 2008.

20. **Levine B, and Yuan J**. Autophagy in cell death: an innocent convict? *The Journal of clinical investigation* 115: 2679-2688, 2005.

21. **Li W, Petrimpol M, Molle KD, Hall MN, Battegay EJ, and Humar R**. Hypoxia-induced endothelial proliferation requires both mTORC1 and mTORC2. *Circulation research* 100: 79-87, 2007.

22. **Mandegar M, Fung YC, Huang W, Remillard CV, Rubin LJ, and Yuan JX**. Cellular and molecular mechanisms of pulmonary vascular remodeling: role in the development of pulmonary hypertension. *Microvascular research* 68: 75-103, 2004.

23. **Mizushima N, Levine B, Cuervo AM, and Klionsky DJ**. Autophagy fights disease through cellular self-digestion. *Nature* 451: 1069-1075, 2008.

24. **Nishimura R, Kawasaki T, Sekine A, Suda R, Urushibara T, Suzuki T, Takayanagi S, Terada J, Sakao S, and Tatsumi K**. Hypoxia-induced proliferation of tissue-resident endothelial progenitor cells in the lung. *American journal of physiology Lung cellular and molecular physiology*

ajplung.00243.02014, 2014.

25. **Ogawa A, Firth AL, Yao W, Madani MM, Kerr KM, Auger WR, Jamieson SW, Thistlethwaite PA, and Yuan JX**. Inhibition of mTOR attenuates store-operated Ca2+ entry in cells from endarterectomized tissues of patients with chronic thromboembolic pulmonary hypertension. *American journal of physiology Lung cellular and molecular physiology* 297: L666-676, 2009.

26. **Oka M, Homma N, Taraseviciene-Stewart L, Morris KG, Kraskauskas D, Burns N, Voelkel NF, and McMurtry IF**. Rho kinase-mediated vasoconstriction is important in severe occlusive pulmonary arterial hypertension in rats. *Circulation research* 100: 923-929, 2007.

27. **Rai PR, Cool CD, King JA, Stevens T, Burns N, Winn RA, Kasper M, and Voelkel NF**. The cancer paradigm of severe pulmonary arterial hypertension. *American journal of respiratory and critical care medicine* 178: 558-564, 2008.

28. **Ranchoux B, Antigny F, Rucker-Martin C, Hautefort A, Pechoux C, Bogaard HJ, Dorfmuller P, Remy S, Lecerf F, Plante S, Chat S, Fadel E, Houssaini A, Anegon I, Adnot S, Simonneau G, Humbert M, Cohen-Kaminsky S, and Perros F**. Endothelial-to-Mesenchymal Transition in Pulmonary Hypertension. *Circulation* 131: 1006-1018, 2015.

29. **Sakao S, Taraseviciene-Stewart L, Lee JD, Wood K, Cool CD, and Voelkel NF**. Initial apoptosis is followed by increased proliferation of apoptosis-resistant endothelial cells. *FASEB journal : official publication of the Federation of American Societies for Experimental Biology* 19: 1178-1180, 2005.

30. **Sakao S, and Tatsumi K**. Vascular remodeling in pulmonary arterial hypertension: multiple cancer-like pathways and possible treatment modalities. *International journal of cardiology* 147: 4-12, 2011.

31. **Sakao S, Tatsumi K, and Voelkel NF**. Endothelial cells and pulmonary arterial hypertension: apoptosis, proliferation, interaction and transdifferentiation. *Respiratory research* 10: 95, 2009.

32. **Sakao S, Tatsumi K, and Voelkel NF**. Reversible or irreversible remodeling in pulmonary arterial hypertension. *American journal of respiratory cell and molecular biology* 43: 629-634, 2010.

33. **Sakao S, Voelkel NF, Tanabe N, and Tatsumi K**. Determinants of an elevated pulmonary arterial pressure in patients with pulmonary arterial hypertension. *Respiratory research* 16: 84, 2015.

34. **Sarbassov DD, Ali SM, Sengupta S, Sheen JH, Hsu PP, Bagley AF, Markhard AL, and Sabatini DM**. Prolonged rapamycin treatment inhibits mTORC2 assembly and Akt/PKB. *Molecular cell* 22: 159-168, 2006.

35. **Schermuly RT, Kreisselmeier KP, Ghofrani HA, Samidurai A, Pullamsetti S, Weissmann N, Schudt C, Ermert L, Seeger W, and Grimminger F**. Antiremodeling effects of iloprost and the dual-selective phosphodiesterase 3/4 inhibitor tolafentrine in chronic experimental pulmonary hypertension. *Circulation research* 94: 1101-1108, 2004.

36. **Shinohara T, Sawada H, Otsuki S, Yodoya N, Kato T, Ohashi H, Zhang E, Saitoh S,**

Shimpo H, Maruyama K, Komada Y, and Mitani Y. Macitentan reverses early obstructive pulmonary vasculopathy in rats: early intervention in overcoming the survivin-mediated resistance to apoptosis. *American journal of physiology Lung cellular and molecular physiology* 308: L523-538, 2015.

37. **Stacher E, Graham BB, Hunt JM, Gandjeva A, Groshong SD, McLaughlin VV, Jessup M, Grizzle WE, Aldred MA, Cool CD, and Tuder RM**. Modern age pathology of pulmonary arterial hypertension. *American journal of respiratory and critical care medicine* 186: 261-272, 2012.

38. **Taraseviciene-Stewart L, Kasahara Y, Alger L, Hirth P, Mc Mahon G, Waltenberger J, Voelkel NF, and Tuder RM**. Inhibition of the VEGF receptor 2 combined with chronic hypoxia causes cell death-dependent pulmonary endothelial cell proliferation and severe pulmonary hypertension. *FASEB journal : official publication of the Federation of American Societies for Experimental Biology* 15: 427-438, 2001.

39. **Toba M, Alzoubi A, O'Neill KD, Gairhe S, Matsumoto Y, Oshima K, Abe K, Oka M, and McMurtry IF**. Temporal hemodynamic and histological progression in Sugen5416/hypoxia/normoxia-exposed pulmonary arterial hypertensive rats. *American journal of physiology Heart and circulatory physiology* 306: H243-250, 2014.

40. **Wharton J, Strange JW, Moller GM, Growcott EJ, Ren X, Franklyn AP, Phillips SC, and Wilkins MR**. Antiproliferative effects of phosphodiesterase type 5 inhibition in human pulmonary artery cells. *American journal of respiratory and critical care medicine* 172: 105-113, 2005.

41. **Zhang XM, Li L, Xu JJ, Wang N, Liu WJ, Lin XH, Fu YC, and Luo LL**. Rapamycin preserves the follicle pool reserve and prolongs the ovarian lifespan of female rats via modulating mTOR activation and sirtuin expression. *Gene* 523: 82-87, 2013.

Figure legends

Fig. 1.

Study design. The outline of the time course study is shown in A. White and black arrowheads indicate the points of evaluation. A black arrowhead indicates the representative point for comparison in the hemodynamic or pathological analysis with the control. The intervention protocol is shown in B. SuHx, Sugen/Hypoxia exposed model.

Fig.2

Time-dependent alterations in the right ventricular systolic pressure (RVSP) (A), right ventricle/left ventricle + septum (RV/LV+S) ratio (B), heart rate (C) and body weight (D). Ctrl, control; wk, week(s) after the SU5416 injection. Statistical analyses were performed using a one-way ANOVA followed by Tukey's multiple comparisons test except for body weight. Values are expressed as the means ± SE. * $p<0.05$ vs. ctrl; † $p<0.05$ vs. 1 wk; ‡ $p<0.05$ vs. 3 wk; § $p<0.05$ vs. 5 wk.

Fig. 3

Time-dependent alterations in the pulmonary arteries.

A: The mean percentage of grade 0 (G0, no evidence of luminal occlusion), grade 1 (G1, < 50% occlusion) and grade 2 (G2, > 50% occlusion) in pulmonary arteries with outer diameters (OD) < 50 μm are shown. B: G2 arteries are additionally classified into the plexiform and non-plexiform types. The mean percentages of plexiform and non-plexiform types in OD < 50 μm arteries for the entire cohort are shown. C: The mean percentages of G0, G1 and G2 in pulmonary arteries of 50 μm < OD < 100 μm are shown. D: The mean percentages of the plexiform and non-plexiform types in 50 μm < OD < 100 μm arteries for the entire cohort are shown. Values are expressed as the means ± SE. Statistical analyses were performed using a one-way ANOVA followed by Tukey's multiple comparisons test. * $p<0.05$ vs. ctrl; † $p<0.05$ vs. 1 wk; ‡ $p<0.05$ vs. 3 wk; § $p<0.05$ vs. 5 wk. E-H: Representative photomicrographs of the pulmonary arteries stained with Elastica van Gieson stain. E, G0; F, G1; G and H, G2. I-L: Representative photomicrographs of the pulmonary arteries stained with von Willebrand factor. I and J, non-plexiform type; K and L, plexiform type. Scale bars = 50 μm.

Fig. 4

Pulmonary vascular endothelial cell (EC) kinetics over the time course in

Sugen/hypoxia (SuHx) rats using flow cytometry (FCM) analyses.

A-D: Representative FCM panels. A: Whole lung cells of ctrl at 1 week (wk) stained with CD31 and CD45 are shown. CD31-positive and CD45-negative cells were defined as ECs. B: LC3-positive ECs from control (Ctrl) or Sugen/Hypoxia rats (3 wk). C: BrdU-positive ECs from ctrl or Sugen/Hypoxia rats (1 wk). D: Nuclear staining of ECs by Hoechst. Gates showed an area of Hoechst < 2n (less than diploidy, defined as apoptotic ECs). E: The mean percentage of LC3-positive ECs. F: The mean percentage of LC3-positive ECs was compared among Ctrl, Sugen/Hypoxia and Hypoxia rats at 3 weeks (wk). G: The mean percentage of BrdU-positive ECs. H: The mean percentage of Hoechst < 2n in ECs. I: The number of ECs/body weight (BW). Values are expressed as the means ± SE. Statistical analyses were performed using Student's *t*-test or a one-way ANOVA followed by Tukey's multiple comparisons test. * $p<0.05$ vs. Ctrl.

Fig. 5

Time-dependent alterations in LC3-positive pulmonary arteries.

A-D: Representative photomicrographs of pulmonary arteries immunostained with LC3. A and B, LC3-positive; C and D, LC3-negative. Scale bars = 50 μm. The mean

percentage of LC3-positive pulmonary arteries. The evaluation of outer diameter (OD) < 50 μm, 50 μm < OD < 100 μm or OD > 100 μm arteries is shown in Fig. E-G, respectively. Values are expressed as the means ± SE. Statistical analyses were performed using a one-way ANOVA followed by Tukey's multiple comparisons test. * $p<0.05$ vs. ctrl.

Fig. 6

The mean percentage of LC3-positive pulmonary arteries was compared among 3 types of outer diameter (OD), OD < 50 μm, 50 μm < OD < 100 μm and OD > 100 μm arteries at the same experimental period. A: Comparison at 1 week. B: Comparison at 3 weeks. Values are expressed as the means ± SE. Statistical analyses were performed using a one-way ANOVA followed by Tukey's multiple comparisons test.

Fig. 7

Effects of rapamycin in the intervention protocol (1).

A-D: Right ventricular systolic pressure (RVSP) (A), heart rate (B), right ventricle/left ventricle + septum (RV/LV+S) ratio (C) and body weight (BW) (D) were compared between rapamycin- and vehicle-treated Sugen/Hypoxia rats at 8 weeks. Rap,

rapamycin-treated Sugen/Hypoxia rats; Veh, vehicle-treated Sugen/Hypoxia rats. E-H: Flow cytometry analyses. The mean percentage of LC3-positive ECs (E), BrdU-positive ECs (F) and Hoechst < 2n ECs (G) and the number of ECs/BW (H) are compared between rapamycin- and vehicle-treated Sugen/Hypoxia rats at 8 weeks. I-K: The rates of LC3-positive arteries assessed with an immunohistological analysis were compared between rapamycin- and vehicle-treated Sugen/Hypoxia rats at 8 weeks. Analyses of OD < 50 μm, 50 μm < OD < 100 μm and OD > 100 μm arteries are shown in Fig. I-K, respectively. Values are expressed as the means ± SE. Statistical analyses were performed using Student's *t*-test. * $p<0.05$. L-O: Representative photomicrographs of pulmonary arteries immunostained with LC3. LC3-negative pulmonary arteries from vehicle-treated Sugen/Hypoxia rats are shown in Fig. L and M. LC3-positive pulmonary arteries from rapamycin-treated Sugen/Hypoxia rats are shown in Fig. N and O. Scale bars = 50 μm.

Fig. 8

Effects of rapamycin in the intervention protocol (2).

A: The mean percentages of grade 0 (G0), grade 1 (G2) and grade 2 (G2) pulmonary arteries of outer diameters (OD) < 50 μm were compared between rapamycin- and

vehicle-treated Sugen/Hypoxia rats at 8 weeks. Rap, rapamycin-treated Sugen/Hypoxia rats; Veh, vehicle-treated Sugen/Hypoxia rats. B: In OD < 50 μm arteries, the mean percentages of plexiform type in G2 arteries were compared between rapamycin- and vehicle-treated Sugen/Hypoxia rats at 8 weeks. C: The mean percentages of G0, G2 and G2 pulmonary arteries of 50 μm < OD < 100 μm were compared between rapamycin- and vehicle-treated Sugen/Hypoxia rats at 8 weeks. D: In 50 μm < OD < 100 μm arteries, the mean percentages of plexiform type in G2 were compared between rapamycin- and vehicle-treated Sugen/Hypoxia rats at 8 weeks. Values are expressed as the means ± SE. Statistical analyses were performed using Student's *t*-test. * $p<0.05$. E-H: Representative photomicrographs of pulmonary arteries stained with EVG are shown. Fig. E and F, lungs from vehicle-treated Sugen/Hypoxia rats; Fig. G and H, lungs from rapamycin-treated Sugen/Hypoxia rats. Scale bars = 50 μm.

Figure 1

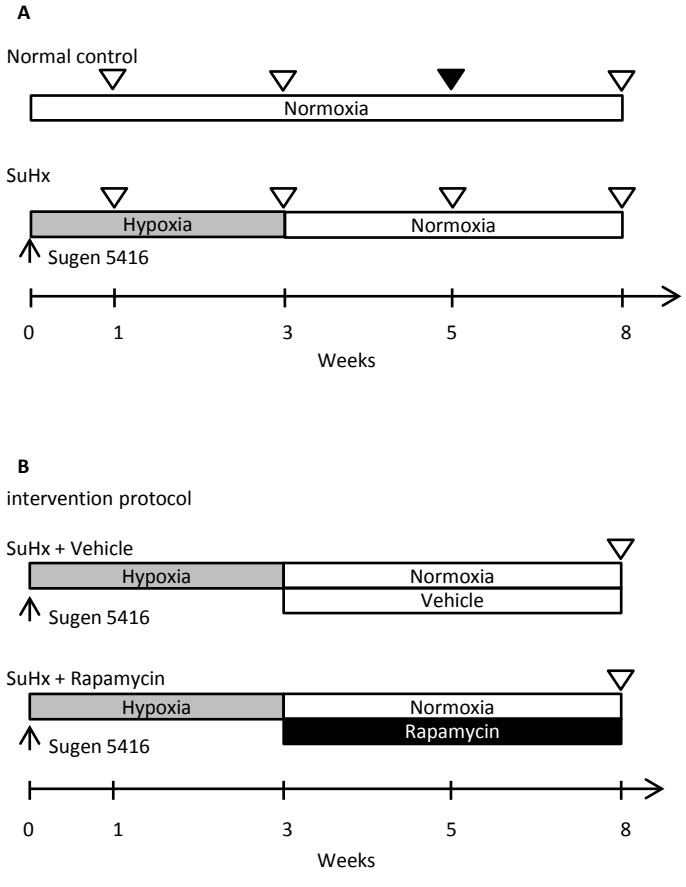
A
Normal control
Normoxia
SuHx
Hypoxia
Normoxia
Sugen 5416
0
1
3
5
8
Weeks
B
intervention protocol
SuHx + Vehicle
Hypoxia
Normoxia
Vehicle
Sugen 5416
SuHx + Rapamycin
Hypoxia
Normoxia
Rapamycin
Sugen 5416
0
1
3
5
8
Weeks

Figure 2

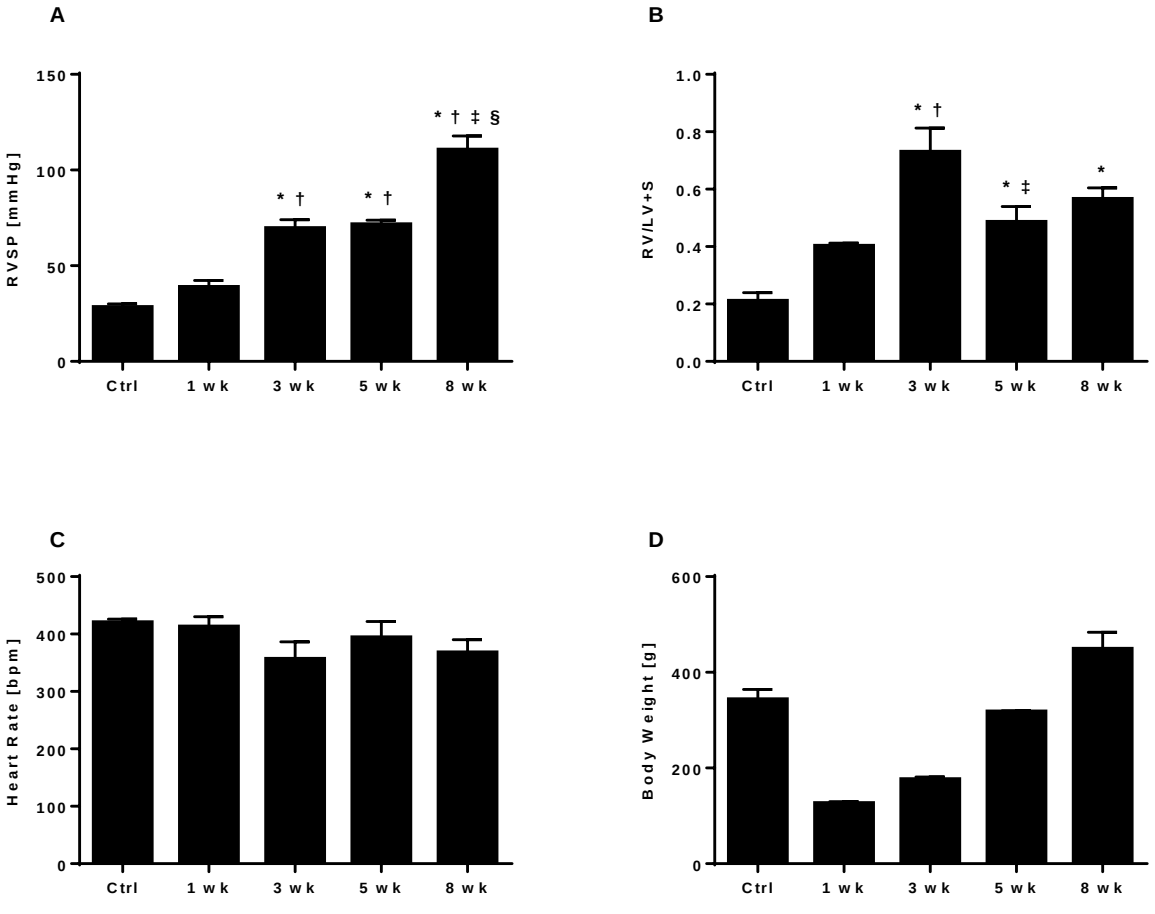
A
RVSP [mmHg]
150
100
50
0
* †
* †
* † ‡ §
Ctrl
1 wk
3 wk
5 wk
8 wk
B
RV/LV+S
1.0
0.8
0.6
0.4
0.2
0.0
* †
* ‡
*
Ctrl
1 wk
3 wk
5 wk
8 wk
C
Heart Rate [bpm]
500
400
300
200
100
0
Ctrl
1 wk
3 wk
5 wk
8 wk
D
Body Weight [g]
600
400
200
0
Ctrl
1 wk
3 wk
5 wk
8 wk

Figure 3-1

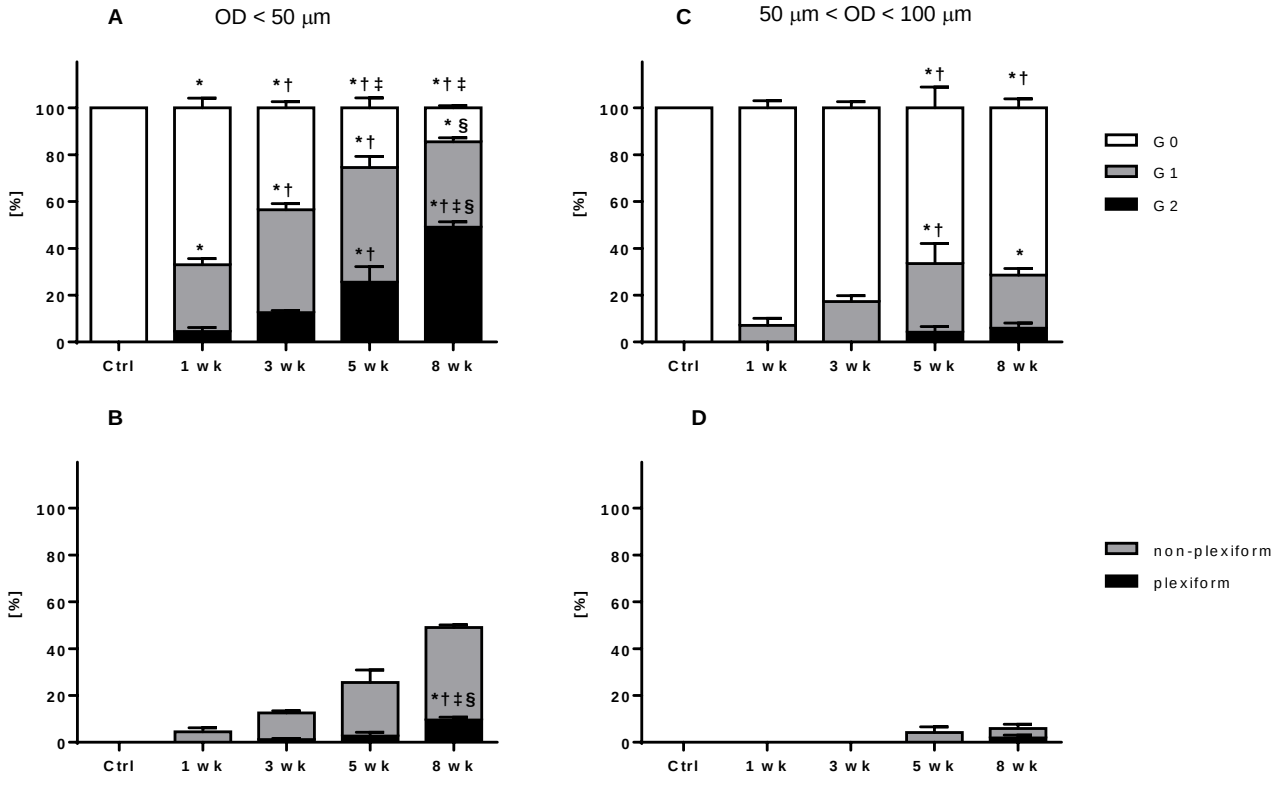
A
OD < 50 μm
C
50 μm < OD < 100 μm
B
D
[%]
Ctrl
1 w k
3 w k
5 w k
8 w k
G 0
G 1
G 2
non-plexiform
plexiform

Figure 3-2

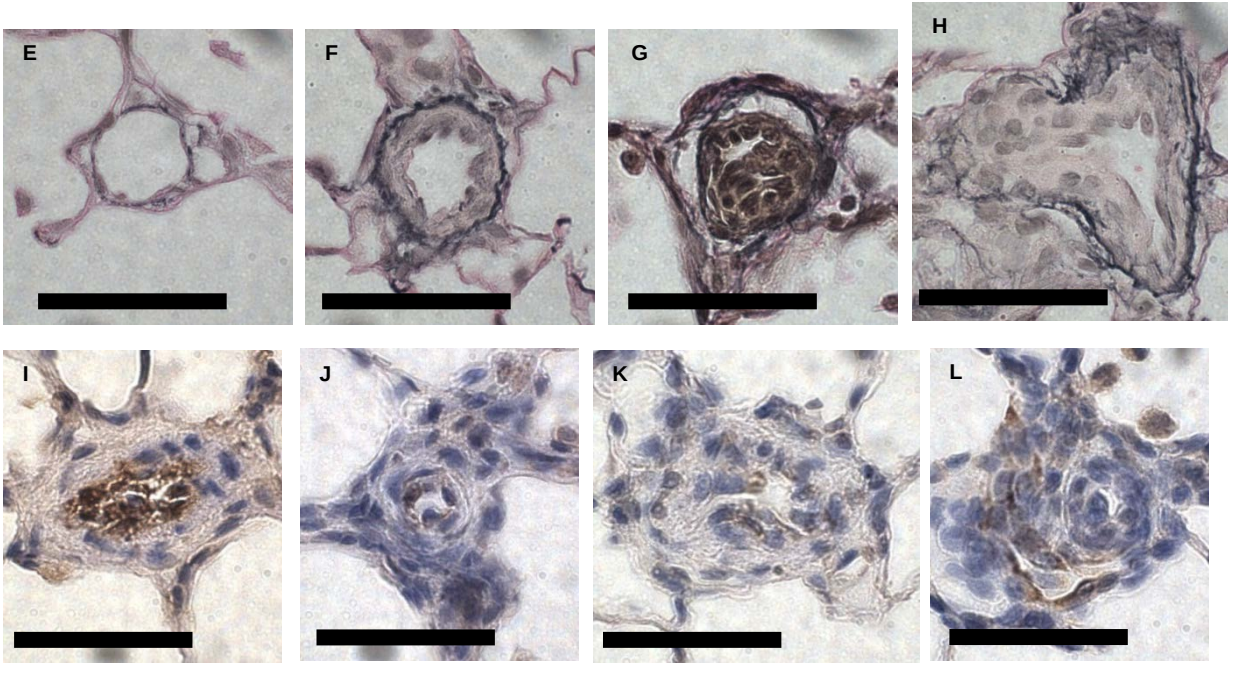

Figure 4-1

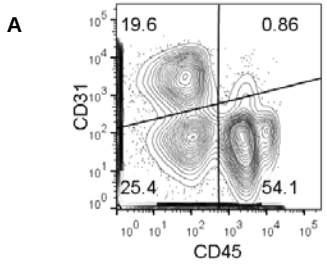
A
19.6
0.86
25.4
54.1
CD31
CD45

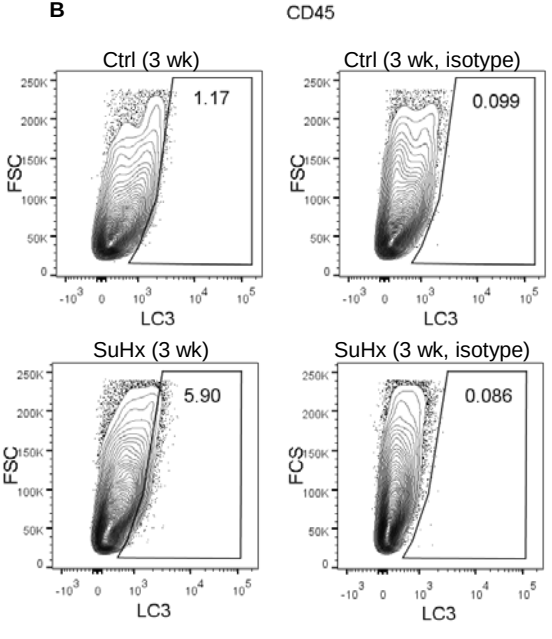
B
Ctrl (3 wk)
1.17
Ctrl (3 wk, isotype)
0.099
SuHx (3 wk)
5.90
SuHx (3 wk, isotype)
0.086
FSC
LC3

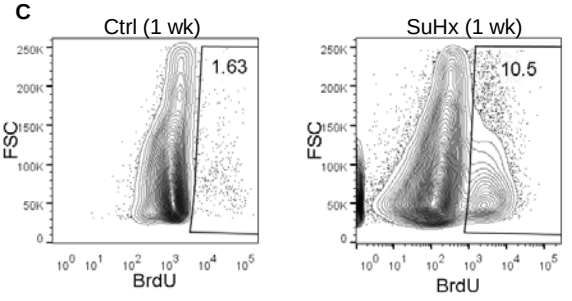
C
Ctrl (1 wk)
1.63
SuHx (1 wk)
10.5
FSC
BrdU

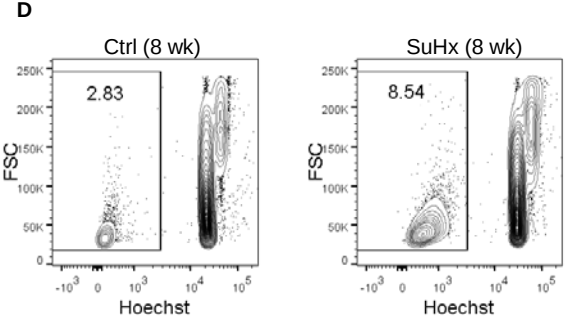
D
Ctrl (8 wk)
2.83
SuHx (8 wk)
8.54
FSC
Hoechst

Figure 4-2

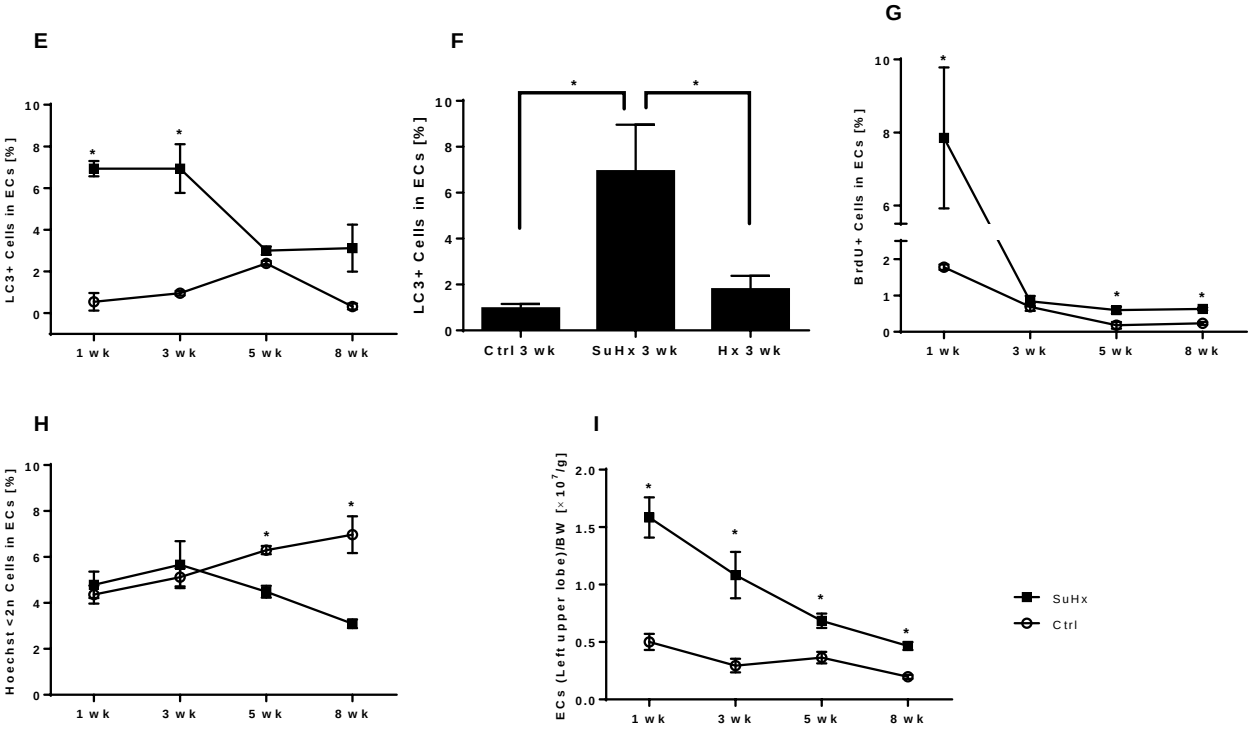
E
LC3+ Cells in ECs [%]
1 wk
3 wk
5 wk
8 wk
F
LC3+ Cells in ECs [%]
Ctrl 3 wk
SuHx 3 wk
Hx 3 wk
G
BrdU+ Cells in ECs [%]
1 wk
3 wk
5 wk
8 wk
H
Hoechst <2n Cells in ECs [%]
1 wk
3 wk
5 wk
8 wk
I
ECs (Left upper lobe)/BW [×10^7/g]
1 wk
3 wk
5 wk
8 wk
SuHx
Ctrl

Figure 5

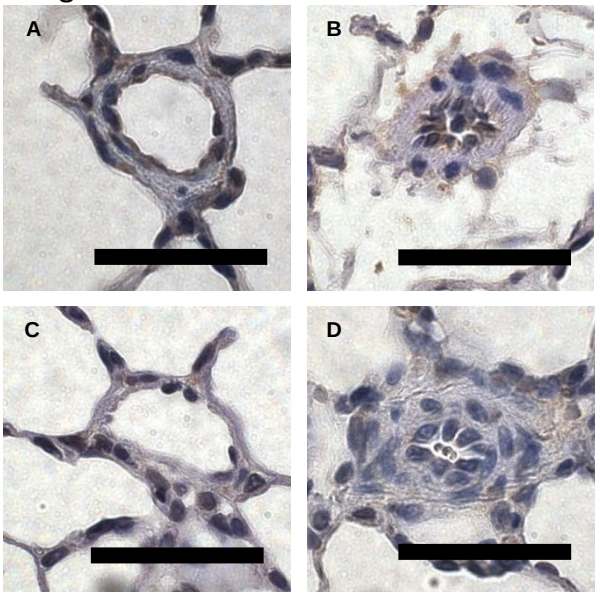
A
B
C
D

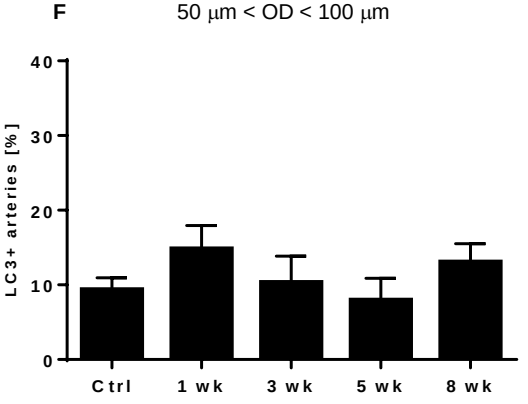
F
50 μm < OD < 100 μm
LC3+ arteries [%]
40
30
20
10
0
Ctrl
1 wk
3 wk
5 wk
8 wk

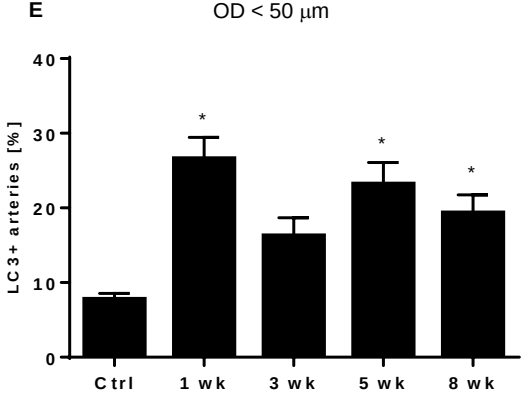
E
OD < 50 μm
LC3+ arteries [%]
40
30
20
10
0
*
*
*
Ctrl
1 wk
3 wk
5 wk
8 wk

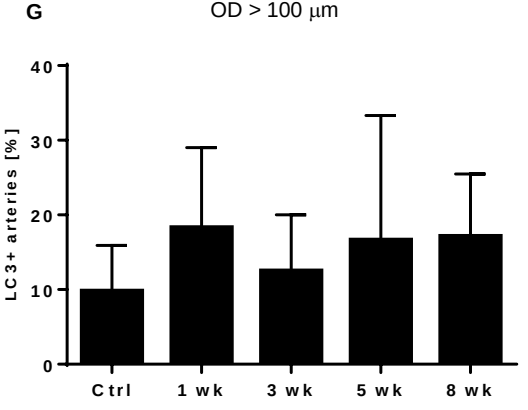
G
OD > 100 μm
LC3+ arteries [%]
40
30
20
10
0
Ctrl
1 wk
3 wk
5 wk
8 wk

Figure 6

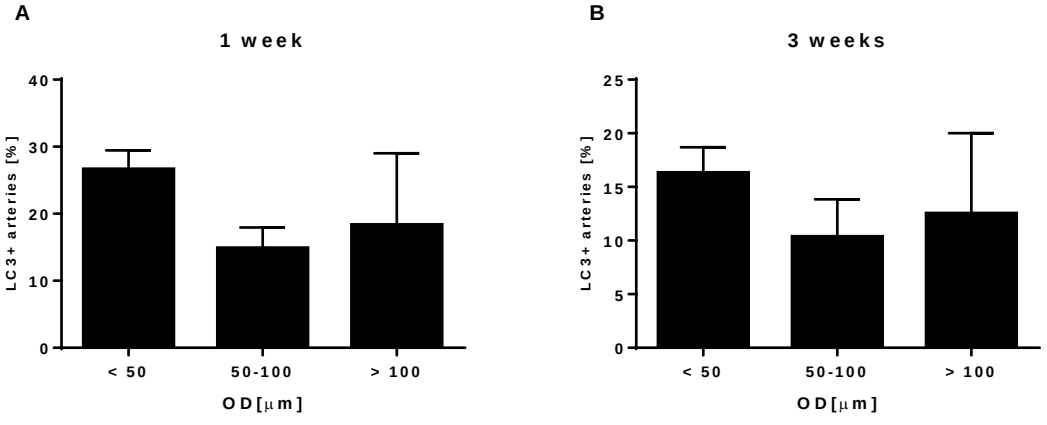
A
1 week
LC3+ arteries [%]
40
30
20
10
0
< 50
50-100
> 100
OD[µm]
B
3 weeks
LC3+ arteries [%]
25
20
15
10
5
0
< 50
50-100
> 100
OD[µm]

Figure 7-1

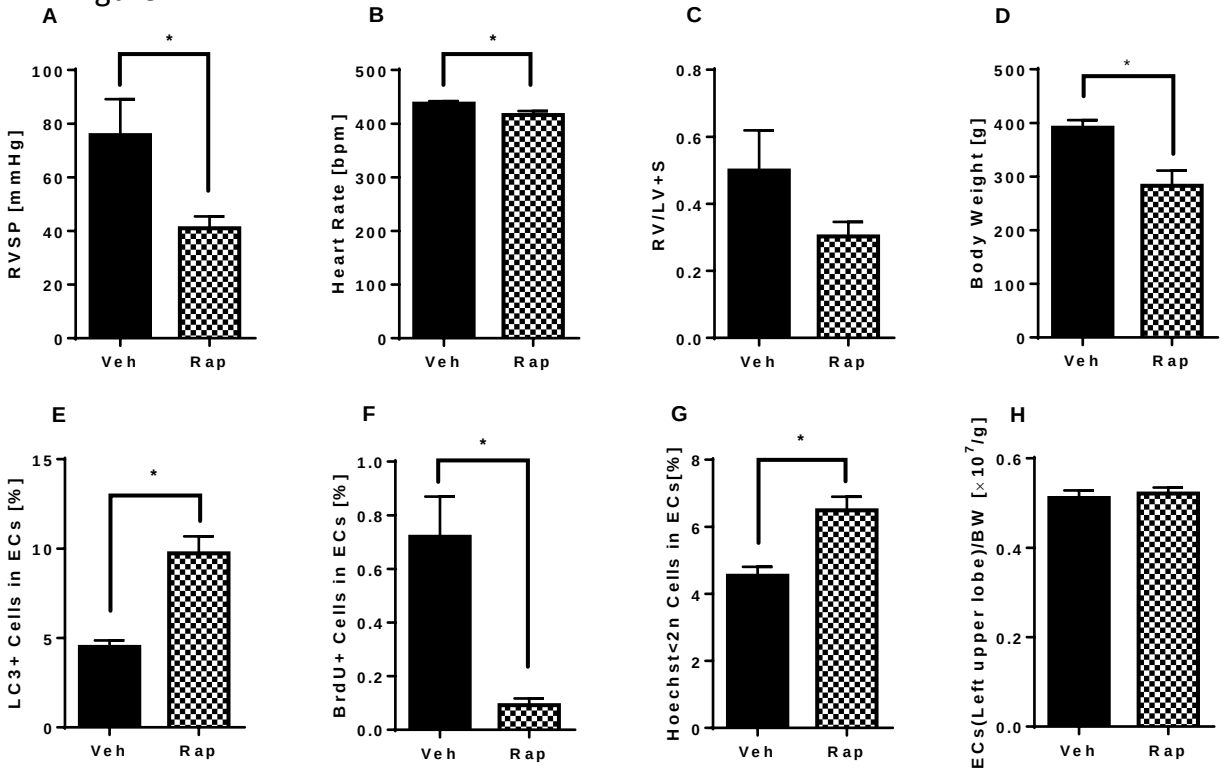
A
RVSP [mmHg]
100
80
60
40
20
0
*
Veh
Rap
B
Heart Rate [bpm]
500
400
300
200
100
0
*
Veh
Rap
C
RV/LV+S
0.8
0.6
0.4
0.2
0.0
Veh
Rap
D
Body Weight [g]
500
400
300
200
100
0
*
Veh
Rap
E
LC3+ Cells in ECs [%]
15
10
5
0
*
Veh
Rap
F
BrdU+ Cells in ECs [%]
1.0
0.8
0.6
0.4
0.2
0.0
*
Veh
Rap
G
Hoechst<2n Cells in ECs[%]
8
6
4
2
0
*
Veh
Rap
H
ECs(Left upper lobe)/BW [×10^7/g]
0.6
0.4
0.2
0.0
Veh
Rap

Figure 7-2

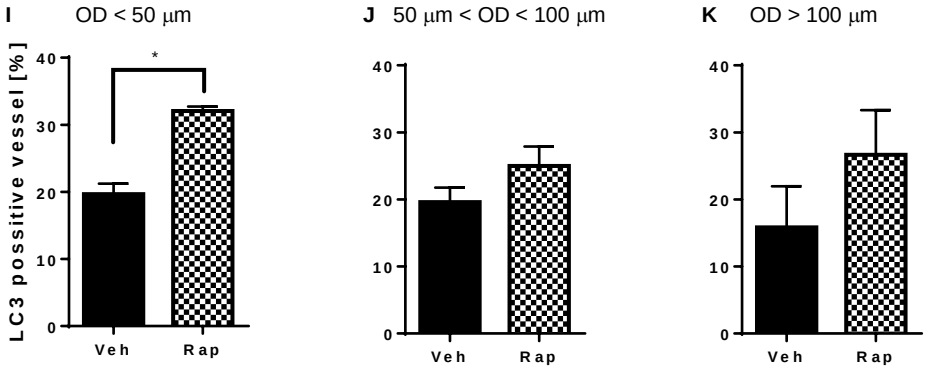

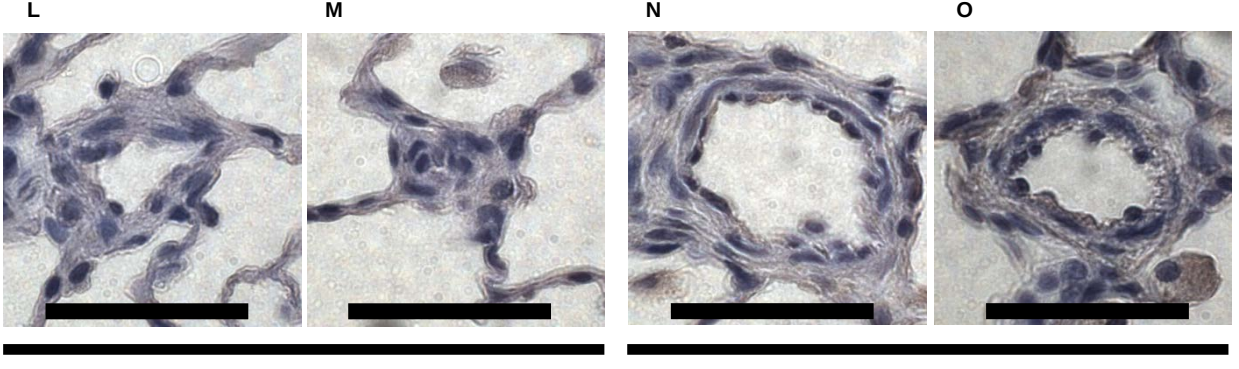

vehicle-treated Sugen/Hypoxia rats

rapamycin-treated Sugen/Hypoxia rats

Figure 8-1

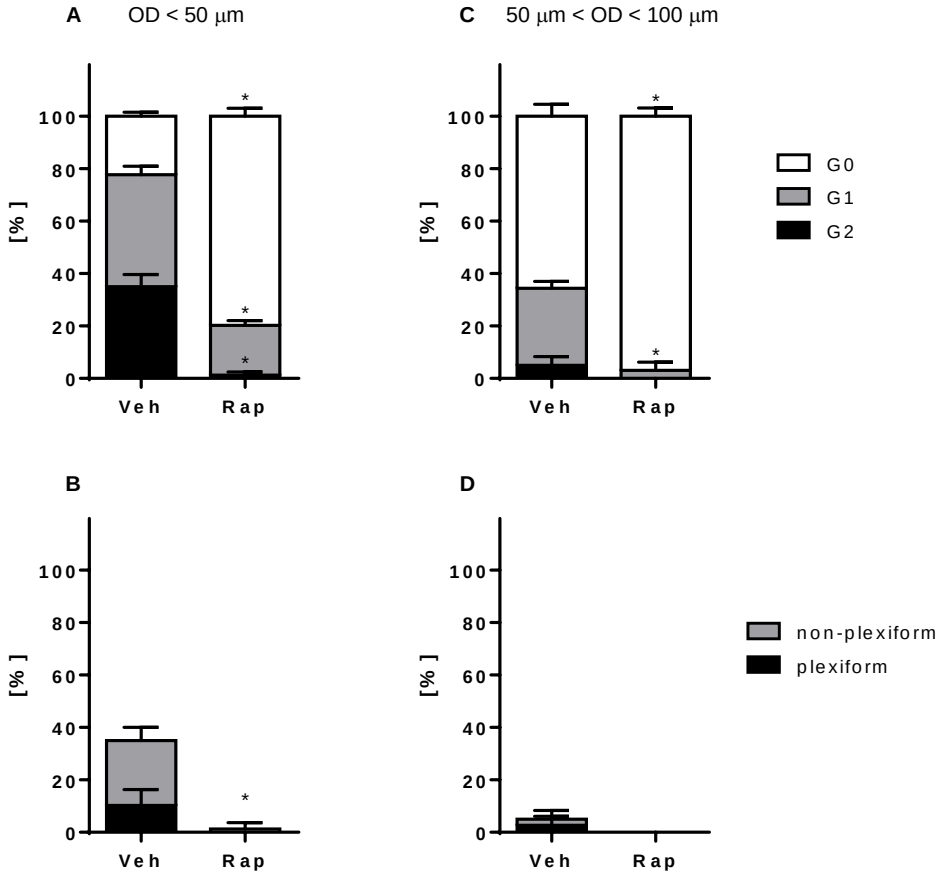
A
OD < 50 μm
C
50 μm < OD < 100 μm
[%]
100
80
60
40
20
0
Veh
Rap
*
G0
G1
G2
B
D
non-plexiform
plexiform

Figure 8-2

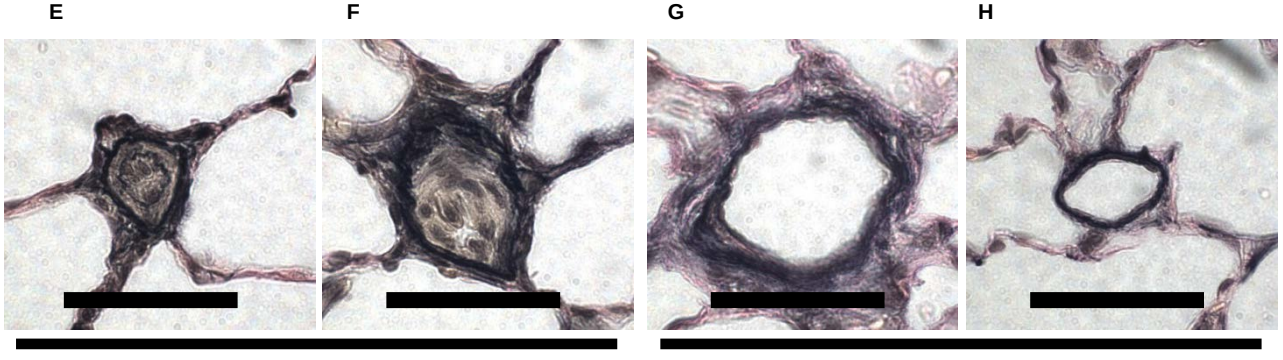

vehicle-treated Sugen/Hypoxia rats

rapamycin-treated Sugen/Hypoxia rats

European Respiratory Journal

平成 **27** 年 **11** 月　投稿中